EurJIC European Journal of Inorganic Chemistry

ChemPubSoc Europe

FULL PAPER

DOI:10.1002/ejic.201402327

Coordination Cluster Analogues of the High-Spin [Mn_{19}] System with Functionalized 2,6-Bis(hydroxymethyl)phenol Ligands

Samir Mameri,*[a][‡] Ayuk M. Ako,*[b,c] Fatma Yesil,[a] Marcel Hibert,[a] Yanhua Lan,[b] Christopher E. Anson,[b] and Annie K. Powell*[b,c]

Keywords: Cluster compounds / Ligand design / Tridentate ligands / Molecular magnetism / Manganese

A series of 2,6-bis(hydroxymethyl)-4-R-phenol ligands (H_3L^R; R = H, F, Cl, Br, I, Ph, NH_2, NO_2, SMe) have either been newly synthesized or the existing syntheses have been significantly improved to investigate ligand-functionalized analogues of the previously published coordination cluster $[Mn^{III}_{12}Mn^{II}_7(\mu_4\text{-}O)_8(\mu_3\text{-}N_3)_8(HL^{Me})_{12}(MeCN)_6]Cl_2\cdot10MeOH\cdot MeCN$ (**1**) with $S = 83/2$. The crystal structures and magnetic properties of three such Mn_{19} clusters, namely, $[Mn^{III}_{12}Mn^{II}_7(\mu_4\text{-}O)_8(HL^H)_{12}(\mu_3\text{-}Cl)_7(\mu_3\text{-}OMe)(MeOH)_6]Cl_2\cdot16H_2O\cdot10MeOH\cdot MeCN$ (**3**), $[Mn^{III}_{12}Mn^{II}_7(\mu_4\text{-}O)_8(HL^I)_{12}(\mu_3\text{-}N_3)_8(MeOH)_6](O_2CH)_2\cdot16MeOH\cdot10MeCN$ (**4**) and $[Mn^{III}_{12}Mn^{II}_7(\mu_4\text{-}O)_8(\mu_3\text{-}Cl)_{7.7}(\mu_3\text{-}OMe)_{0.3}(HL^{SMe})_{12}(MeOH)_6]Cl_2\cdot27MeOH$ (**5**) are reported and compared to those of the parent cluster. When these ligands are functionalized with substituents of moderate electronegativity, it is possible to synthesize Mn_{19} analogues; however, when such ligands bear highly electron-donating (amino) or -withdrawing (nitro) substituents, the Mn_{19} analogues are no longer accessible. The Mn_{19} cluster framework is both magnetically and structurally robust with respect to the electron-donor/acceptor characteristics of the ligand substituent; therefore, the Mn_{19} system is an excellent platform for peripheral chemical engineering.

Introduction

The design and synthesis of molecular materials with predictable magnetic properties continues to remain a challenging task, because the structural factors that govern exchange coupling between paramagnetic centres are complex and elusive. Previously, we reported the [Mn_{19}] coordination cluster $[Mn^{III}_{12}Mn^{II}_7(\mu_4\text{-}O)_8(\mu_3\text{-}\eta^1\text{-}N_3)_8(HL^{Me})_{12}(MeCN)_6]Cl_2\cdot10MeOH\cdot MeCN$ (**1**), which was synthesized from the commercially available 2,6-bis(hydroxymethyl)-4-methylphenol (H_3L^{Me}). The coordination cluster **1** can be described in terms of its central inorganic $\{Mn^{III}_{12}Mn^{II}_7(\mu_4\text{-}O)_8\}$ core, which is formed from the fusion of two supertetrahedral $\{Mn^{III}_6Mn^{II}_4\}$ units that share a common Mn^{II} vertex. The core is then encapsulated within a coordination shell made up of 12 organic ligands and eight face-bridging μ_3,η^1-X (e.g., X = azide) ligands. In this coordination cluster, the ferromagnetic coupling of all of the $Mn^{II/III}$ centres leads to the record ground spin state of $S = 83/2$,[1] which was further corroborated by EPR spectroscopy[2] and DFT calculations.[3]

The 4-substituted H_3L^R ligand system based on 2,6-bis(hydroxymethyl)phenol (Scheme 1) employed in the synthesis of **1** is quite appealing for a number of reasons,[1,4] though its use in coordination chemistry has been quite limited.[1,5,6] For instance, when partially or completely deprotonated, the phenolic and two hydroxy groups of the H_3L^R ligand system have the capacity to bridge three metal ions in a linear fashion, and the relatively short distances between those metal ions could favour ferromagnetic exchange pathways. Given the very large ground-state spin of **1**, a natural extension to our previous work on the [Mn_{19}]

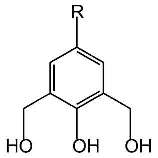

Scheme 1. Chemical structure of ligands based on 2,6-bis(hydroxymethyl)-4-R-phenol, H_3L^R; R = Me, H, Cl, Br, F, I, NH_2, NO_2, SMe and OMe.

---

[a] Laboratoire d'Innovation Thérapeutique (Medicinal Chemistry Laboratory), University of Strasbourg, UMR 7200-CNRS, Faculté de Pharmacie,
74, route du Rhin, 67401 Illkirch, France
http://medchem.u-strasbg.fr/pages/welcome.php
[b] Institut für Anorganische Chemie, Karlsruhe Institute of Technology (KIT),
Engesserstr. 15, 76131 Karlsruhe, Germany
E-mail: annie.powell@kit.edu
manase.ayuk@kit.edu
http://www.aoc.kit.edu/
[c] Institute of Nanotechnology, Karlsruhe Institute of Technology (KIT),
P. O. Box 3640, 76021 Karlsruhe, Germany
http://www.int.kit.edu/home.php
[‡] Current address: Institut de Chimie, UMR 7177/CNRS-Unistra, University of Strasbourg, 4, rue Blaise Pascal, 67000 Strasbourg, France
E-mail: mameri@unistra.fr

system is the use of analogous ligands in which the 4-methyl substituent of the H_3L^{Me} ligand system is replaced by other R groups. Such functionalization could be aimed at further chemical elaboration of the system. For example, the $–NH_2$ group was targeted as a gateway to other functionalities such as peptides or for C–N amination cross-coupling reactions, and the ligand bearing a pendant iodo end group is a good candidate for cross-coupling reactions in solution or solid state. Alternatively, a substituent may aid the interaction of the cluster with a substrate. To this effect, we recently demonstrated the use of the ligand H_3L^{OMe} in the synthesis of the Mn_{19} aggregate $[Et_3NH]_2[Mn^{III}_{12}Mn^{II}_7(\mu_4\text{-}O)_8(\mu_3\text{-}N_3)_{7.4}(\mu_3\text{-}Cl)_{0.6}(HL^{OMe})_{12}(MeOH)_6]Cl_4\cdot 14MeOH$ (**2**), molecules of which were successfully deposited onto highly oriented pyrolytic graphite (HOPG) substrates and investigated by scanning tunneling microscopy (STM) and current imaging tunneling spectroscopy (CITS).[4] A sulfur-based substituent such as $–SCH_3$ would allow attachment of the cluster to the surfaces of metals such as gold.[7] As changes to the electron-donor/acceptor properties of the *para* substituent will alter the electron density of the bridging phenoxo group within the ligand, it is essential to know whether the core structure of the $[Mn_{19}]$ aggregates as well as their magnetic properties are retained upon ligand functionalization, before any further manipulation and investigation. High-spin isotropic molecules are also of interest because of their potential for applications that utilize their magnetocaloric effect, for example, in refrigeration or in theranostics, for which such complexes could be used as magnetic resonance imaging contrast agents.[8,9] Convenient syntheses of the ligands H_3L^{Cl}, H_3L^{Ph} and H_3L^{OMe} are already readily available, but those published for H_3L^{F}, H_3L^{Br}, H_3L^{H}, H_3L^{I} and $H_3L^{NO_2}$ are more problematic and often require large-scale column chromatography.[10] In this paper, we expand on our earlier work by reporting improved and optimized syntheses of the latter five ligands and describe the syntheses of the new compounds $H_3L^{NH_2}$ and H_3L^{SMe}. We then describe the syntheses, structures and magnetic properties of the $[Mn_{19}]$ aggregates derived from three of these ligands (H_3L^{H}, **3**; H_3L^{I}, **4**; H_3L^{SMe}, **5**) and compare these with the aggregates involving the ligands with R = Me[1] and OMe.[4]

Results and Discussion

Synthetic Studies

Previously, we reported the Mn_{19} aggregate $[Mn^{III}_{12}Mn^{II}_7(\mu_4\text{-}O)_8(\mu_3\text{-}N_3)_8(HL^{Me})_{12}(MeCN)_6]Cl_2\cdot 10MeOH\cdot MeCN$ (**1**), which displays the highest spin ground state known for a 3d molecular species to date: $S_T = 83/2$.[1] The organic ligand $(HL^{Me})^{2-}$ in this complex is obtained by deprotonation of the commercially available 2,6-bis(hydroxymethyl)-4-methylphenol (H_3L^{Me}). It was considered useful to prepare analogous aggregates with ligands bearing alternative functional groups at the 4-position. Although the published syntheses of the ligands H_3L^{Cl} and H_3L^{OMe} are relatively convenient, those for H_3L^{H}, H_3L^{F}, H_3L^{Br}, H_3L^{I} and $H_3L^{NO_2}$ are not. The fluoro and bromo ligands, in particular, require time-consuming large-scale column chromatography.[10] Our modified syntheses of the H_3L^{Br} and H_3L^{F} ligands were realized by treating the corresponding *para*-substituted phenols with formaldehyde in basic

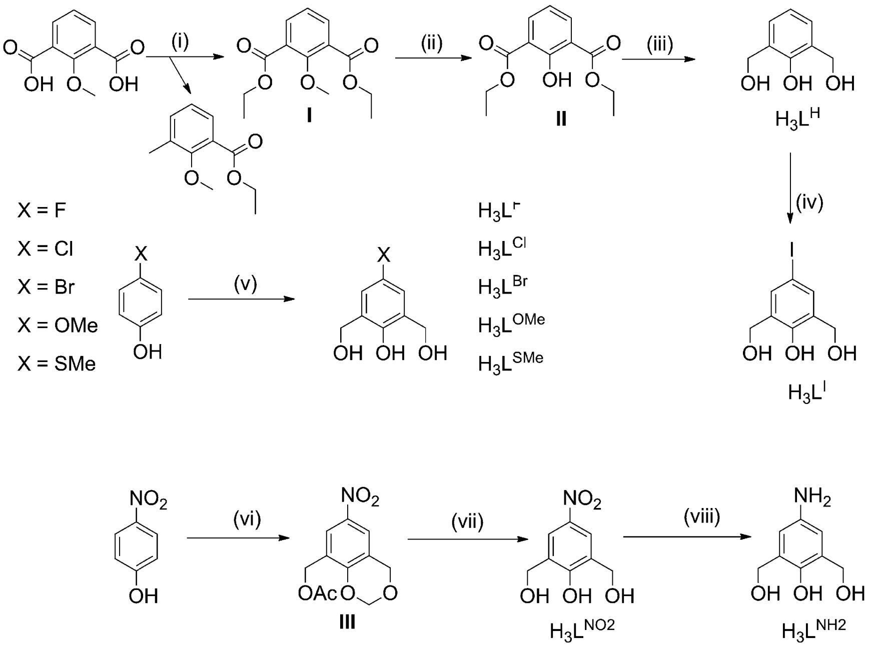

Scheme 2. Synthetic scheme for preparation of 2,6-bis(hydroxymethyl)-4-R-phenol ligands H_3L^R. Reagents and conditions: (i) EtOH, H_2SO_4, reflux; (ii) BBr_3, CH_2Cl_2, –78 °C; (iii) $LiAlH_4$, tetrahydrofuran (THF), 0 °C to room temp.; (iv) $BTMA\cdot ICl_2$, $NaHCO_3$, MeOH, room temp.; (v) formaldehyde, NaOH, H_2O/MeOH, Δ; (vi) paraformaldehyde, AcOH, H_2SO_4, 50 °C; (vii) conc. HCl, water, reflux; (viii) H_2, Pd/C, 60 psi, room temp.

media, and the workup for these two ligands was also optimized. The new methylmercapto ligand H_3L^{SMe} could be prepared in a similar way. However, similar reactions involving 4-iodo-, 4-nitro- and 4-aminophenols failed to produce isolable materials (with at best only traces observable by HPLC for the iodo compound). Therefore, we explored new synthetic routes (Scheme 2).

Access to both the parent ligand H_3L^H and the iodo-substituted ligand H_3L^I was made possible by a multistep synthesis from commercially available 2-methoxyisophthalic acid. The product of the first step of this synthesis, diethyl-2-methoxyisophthalate (**I**), was prepared in high yield (ca. 90 %) from 2-methoxyisophthalic acid by using H_2SO_4 for activation. The removal of the methyl group of the anisole methoxy group with BBr_3 to give the corresponding phenol (compound **II**) was quantitative in dry CH_2Cl_2 at –78 °C. A hydride reduction of the ester groups of **II** was then successfully performed to afford the unsubstituted parent ligand H_3L^H. This could then be readily iodinated with benzyltrimethylammonium dichloroiodate ($BTMA\cdot ICl_2$) in the presence of $NaHCO_3$ to yield H_3L^I.[10]

For the synthesis of the amino-substituted ligand $H_3L^{NH_2}$, we first synthesized the benzodioxene derivative 8-acetoxymethyl-6-nitro-1,3-benzodioxene (**III**) from *p*-nitrophenol by using paraformaldehyde under acidic conditions.[10d,10e] Notably, the temperature must be carefully controlled to obtain good yields of dioxene **III**; even a small deviation of a few degrees from the optimal +50 °C led to side-products. Subsequently, the dioxene was heated to reflux in acidic media to free the alcoholic chelating moiety and, thus, afford the nitro ligand $H_3L^{NO_2}$. Finally, a palladium-catalyzed reduction of the nitro group in $H_3L^{NO_2}$ with H_2 under high pressure was then performed to give the new diformylated amino species $H_3L^{NH_2}$. The chemical structures of all of the ligands from our syntheses were confirmed by ^1H, ^{13}C and ^{19}F NMR (for H_3L^F) spectroscopy, high-resolution mass spectroscopy (HRMS) and elemental analysis.

To exploit the broad application of the H_3L^R ligand system and to test the robustness of the [Mn_{19}] system to changes in ligand substituent, we have investigated the ligands in the synthesis of the corresponding [$Mn_{19}R$] aggregates. Of the ligands for which the syntheses are reported here, we describe the structures of the Mn_{19} aggregates obtained with H_3L^H (the unsubstituted "parent" ligand), H_3L^I (as the iodo substituent should allow further ligand functionalization) and H_3L^{SMe} (as the sulfur-containing substituent will allow addressing onto gold surfaces). The synthesis and structure of the complex $[Et_3NH]_2[Mn^{III}_{12}Mn^{II}_7(\mu_4\text{-}O)_8(\mu_3\text{-}N_3)_{7.4}(\mu_3\text{-}Cl)_{0.6}(HL^{OMe})_{12}(MeOH)_6]Cl_4\cdot 14MeOH$ (**2**) has been reported elsewhere.[4] This bears a moderately electron-donating methoxy substituent at the ligand 4-position (Hammett σ_{para} = –0.27, compared to –0.17 for the methyl group in the original aggregate **1**).[11] Similarly, we have previously reported the heterometallic aggregate $[Mn^{III}_{12}Mn^{II}_6Lu^{III}(\mu_4\text{-}O)_8(\mu_3\text{-}\eta^1\text{-}N_3)_6(\mu_3\text{-}\eta^1\text{-}Cl)_2(HL^F)_{12}(MeCN)_6]Cl_3\cdot 3H_2O\cdot 7MeOH\cdot MeCN$,[12] in which the fluoro substituent on the ligand has Hammett σ_{para} = +0.06.[11]

Although the syntheses of the complexes reported here were generally similar to that reported for **1**,[1] the establishment of the appropriate conditions in each case was not straightforward and represented quite a substantial synthetic and crystallization challenge, as had been the case for **2**.[4] In general, the complexes described in this work were obtained upon reaction of the appropriate H_3L^R ligand with a base ($NaOAc\cdot 3H_2O$ or Et_3N) and $MnCl_2\cdot 4H_2O$ or $MnBr_2\cdot 4H_2O$ in the presence or absence of NaN_3 in MeCN/MeOH (typically 5:1 v/v) mixtures and crystallized by slow evaporation of the mother liquor at room temperature. Various reaction conditions such as reaction components, stoichiometry, concentration, reaction time, pH and temperature were investigated, and we report here the optimum conditions that we have established. For instance, with H_3L^H, the Mn_{19} $[Mn^{III}_{12}Mn^{II}_7(\mu_4\text{-}O)_8(\mu_3\text{-}Cl)_7(\mu_3\text{-}OMe)(HL^H)_{12}(MeOH)_6]Cl_2\cdot 16MeOH\cdot MeCN$ (**3**) complex could only be obtained under ambient conditions when Et_3N was employed as a base and in the absence of NaN_3; the synthesis is sensitive to concentration and requires very dilute solutions. By contrast, crystalline products involving H_3L^I could only be obtained from reactions involving NaN_3 under reflux conditions to yield $[Mn^{III}_{12}Mn^{II}_7(\mu_4\text{-}O)_8(\mu_3\text{-}N_3)_8(HL^I)_{12}(MeOH)_6](O_2CH)_2\cdot 16MeOH\cdot 10MeCN$ (**4**). On the other hand, the ligand H_3L^{SMe} required similar reaction conditions to those used for **3** and yielded $[Mn^{III}_{12}Mn^{II}_7(\mu_4\text{-}O)_8(\mu_3\text{-}Cl)_{7.7}(\mu_3\text{-}OMe)_{0.3}(HL^{SMe})_{12}(MeOH)_6]Cl_2\cdot 27MeOH$ (**5**).

Attempted syntheses using the nitro-substituted ligand $H_3L^{NO_2}$ only gave a crystalline product after extended reaction times, and the small crystal size meant that synchrotron radiation was necessary to obtain a good-quality dataset. Initial crystallographic analysis showed that the temperature factor for the central metal ion of the nonadecanuclear complex obtained was significantly higher than those for the other Mn centres (unlike the other Mn_{19} systems we have structurally characterized to date), which indicates that this position is not purely occupied by Mn^{II} ions. Refinement of this metal atom position as a disordered overlay of Mn and Na ions supported this and gave relative occupancies of ca. 80:20 for Mn and Na; this complex was not investigated further. It is unclear whether this Mn/Na mixture at the central position is directly related to the highly electron-withdrawing nitro group on the ligand (Hammett σ_{para} = +0.78[14]) or whether the longer reaction times that were necessary with this ligand are also responsible. No crystalline product was obtained with the strongly electron-donating (Hammett σ_{para} = –0.66[11]) ligand $H_3L^{NH_2}$. Therefore, we conclude that isostructural Mn_{19} aggregates can be synthesized with a wide range of R substituents on the organic ligand, providing the most strongly electron-donating or -withdrawing functional groups (amino or nitro) are avoided.

Structures of the Mn_{19} Aggregates

The structures for **3**–**5** were determined by X-ray diffraction studies (Figure 1), and the crystallographic data are

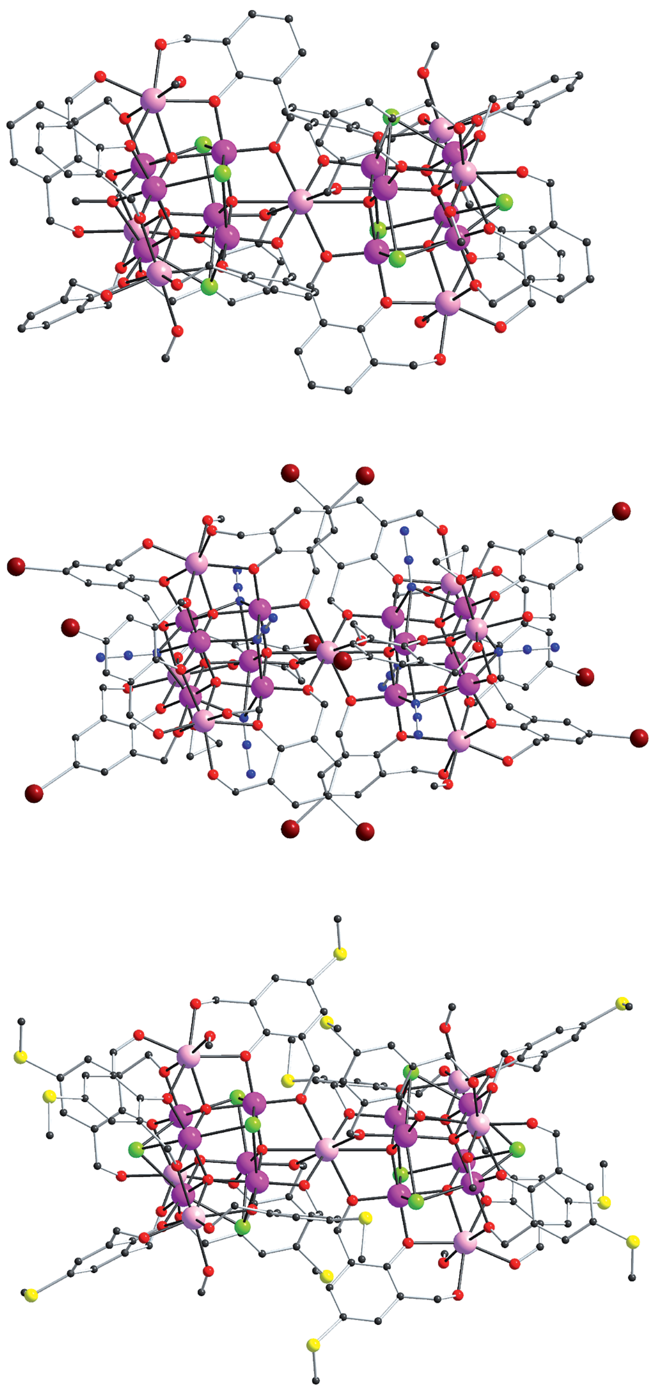

Figure 1. Molecular structures of the Mn_{19} clusters in **3** (top), **4** (middle) and **5** (bottom). H atoms, counterions and lattice solvent molecules omitted for clarity; Mn^{III} dark pink, Mn^{II} pale pink, O red, N blue, Cl green, F pale green, I dark brown.

summarized in Table 3. The structures of these compounds are all very similar to those observed previously for the $[Mn_{19}]$ coordination clusters **1** and **2**.[1,4] As noted in the Introduction, such coordination clusters can be described in terms of a central inorganic $\{Mn^{III}_{12}Mn^{II}_7(\mu_4\text{-}O)_8\}$ core formed from the fusion of two supertetrahedral $\{Mn^{III}_6Mn^{II}_4\}$ units, in which the Mn^{II} centres describe the tetrahedra and share a common Mn^{II} vertex and each has an octahedron of Mn^{III} centres inscribed within them linked by the $\mu_4\text{-}O^{2-}$ bridges. This inorganic core is encapsulated within a coordination shell made up of 12 organic ligands and eight $\mu_3,\eta^1\text{-}X$ ($X = N_3^-$, Cl^- or $-OMe^-$) ligands, which cap the faces of the Mn^{III}_6 octahedra. The three metal centres ($Mn^{II}\cdots Mn^{III}\cdots Mn^{II}$) along each supertetrahedral edge are bridged by two oxygen atoms of the phenoxo group and one alkoxo group, whereas the second alkoxy oxygen remains protonated and ligates the outer Mn^{II} centres (Scheme 3). The differences between these three structures, and also those of **1** and **2**, involve the R substituent of the organic ligand, the $(\mu_3\text{-}X)^-$ face-bridging ligands and, in one case (**4**), the counterions.

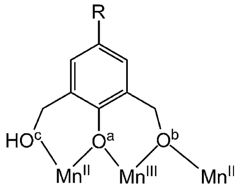

Scheme 3. Coordination of $(HL^R)^{2-}$ ligands (see Table 1). In ligands of type A, O^b coordinates to the central Mn^{II} ion; for ligands of type B, O^b coordinates to an apical Mn^{II} ion.

Aggregate **3** crystallizes in space group $R\bar{3}$ with $Z = 3$; the cell parameter a is similar to that for **1**, but c is somewhat longer, which is perhaps unexpected as the methyl groups in **1** have been replaced by smaller hydrogen atoms in **3**. Although the face-bridging ligands are different (seven chlorido and one methoxo in **3** instead of the eight azides in **1**) the terminal ligands on the outer Mn^{II} centres are now MeOH instead of MeCN, and it appears that the extra hydrogen-bonding capabilities that these provide have resulted in the longer unit cell for **3**. A similar effect was found for the structure of **2**, which also has terminal MeOH ligands.[4] Complex **5** crystallizes in the cubic space group $Pa\bar{3}$ with $Z = 4$, and the crystallographic site symmetry is therefore once again $\bar{3}$ but with a more open crystal structure than for **1**–**3** and a significantly higher lattice solvent content.

By contrast, **4** crystallizes in space group $P2_1/n$ with $Z = 2$ and is, thus, the only compound from **1**–**5** not to crystallize with $\bar{3}$ site symmetry. Although the 4-iodo substituent is substantially larger than most of the others, the different packing is in this case driven by the change in counterion. Instead of chloride ions, as for the other compounds, the charge of the aggregate in **4** is balanced by two formate ions, which presumably result from oxidation of methanol solvent molecules. Each formate ion acts as a supramolecular bridge between two cluster molecules and accepts two hydrogen bonds from each of them.

The principal focus of the work presented here is to study the effect of variation of the substituents on the organic ligands on the properties of the corresponding aggregates. For these purposes, it is convenient to quantify the electron-donating or -withdrawing properties of the various R groups in terms of their Hammett σ_{para} parameters.[11] The bond lengths and angles involving the oxygen atoms of

Table 1. Bond lengths [Å] and angles [°] involving oxygen atoms of the $(HL^R)^{2-}$ ligands in **1**–**5**.[a]

	1[1]	**2**[4]	**3**	**4**[a]	**5**
R	Me	OMe	H	I	SMe
Hammett σ_{para}[11]	–0.17	–0.27	–	+0.18	0.00
μ_3 ligands	$(N_3)_8$	$(N_3)_{7.4}(Cl)_{0.6}$	$(Cl)_7(OMe)$	$(N_3)_8$	$(Cl)_{7.7}(OMe)_{0.3}$
Type A Ligands[b]					
O^a–Mn^{II}	2.2862(17)	2.353(3)	2.306(3)	2.302(4)	2.316(3)
Mn^{II}–O^a–Mn^{III}	103.76(7)	101.41(12)	102.63(12)	102.51(18)	101.70(11)
O^a–Mn^{III}	1.8944(17)	1.891(3)	1.891(3)	1.897(4)	1.905(2)
O^b–Mn^{III}	1.8545(18)	1.854(3)	1.842(3)	1.850(4)	1.848(2)
Mn^{III}–O^b–Mn^{II}	109.29(8)	110.64(13)	110.04(12)	109.6(2)	111.22(10)
O^b–Mn^{II}	2.3446(17)	2.315(3)	2.304(3)	2.332(4)	2.309(2)
O^c–Mn^{II}	2.221(2)	2.187(3)	2.191(3)	2.214(5)	2.216(4)
Type B Ligands[b]					
O^a–Mn^{II}	2.3602(17)	2.325(3)	2.364(3)	2.366(5)	2.334(3)
Mn^{II}–O^a–Mn^{III}	101.27(7)	100.78(12)	104.75(14)	101.8(2)	102.08(11)
O^a–Mn^{III}	1.8947(17)	1.905(3)	1.900(3)	1.896(4)	1.902(3)
O^b–Mn^{III}	1.8782(17)	1.876(3)	1.872(3)	1.874(5)	1.872(3)
Mn^{III}–O^b–Mn^{II}	104.75(8)	104.17(13)	101.57(12)	104.8(2)	104.66(12)
O^b–Mn^{II}	2.1856(17)	2.204(3)	2.188(3)	2.216(5)	2.216(3)
O^c–Mn^{II}	2.211(2)	2.232(3)	2.218(4)	2.199(5)	2.215(3)

[a] For **4**, the parameters given are each the mean value of the three corresponding chemically equivalent but crystallographically independent bond lengths or angles. [b] : Type A ligands bridge a supertetrahedral edge involving the central Mn^{II} ion [Mn(1)] and an "outer" Mn^{II} ion. Type B ligands bridge supertetrahedral edges between two "outer" Mn^{II} centres.

these ligands in **1**–**5** are compared in Table 1. As the atomic numbering schemes are not the same for all of the complexes, the ligand oxygen atoms are designated according to Scheme 3. Within each structure, there are two distinct types of ligand. Although both types have the same connectivity as shown in Scheme 3, six ligands per aggregate bridge edges of a supertetrahedron that link the central Mn^{II} ions [Mn(1) in each structure] to an outer Mn^{II} ion, whereas the other six bridge edges between two outer Mn^{II} centres; these are designated Types A and B, respectively, in Table 1.

In **1**–**5**, it is not only the organic R group that changes; in **1**, **2** and **4**, the face-bridging ligands are all or mostly all azide ligands, whereas they are predominantly chloride ligands in **3** and **5**. However, consideration of the parameters presented in Table 2 should allow us to attribute the effects of the various structural changes. Any direct effect on the ligand–cluster bonding resulting from changes in the R group are likely to result primarily in changes to the geometries around the phenoxo oxygen atoms O^a, that is, Mn^{III}–O^a and Mn^{II}–O^a, as the methanolic oxygen atoms O^b and O^c are not in conjugation with R. Changes resulting from the face-bridging ligands, on the other hand, would result in changes to the Mn^{III}–O^a and Mn^{III}–O^b geometries. However, although some sets of corresponding parameters in Table 1 do show differences at the 3σ significance level, it is not really possible to discern any overall trends that can be assigned to changes in R or the face-bridging ligands. What appears to be the case here is that neither changing the ligand substituent nor the nature of the face-bridging ligand has any significant effect on the Mn–O bonding in terms of the observed bond lengths or angles. We note here that the DFT calculations performed on **1** suggested that the nature of the face-bridging ligands is not the decisive factor governing the magnetic coupling within the aggregate, but rather it is the bonding parameters involving the μ_4-O bridges that govern the overall magnetic structure of the aggregate.[3]

Table 2. Summary of magnetic data for **3**–**5**.

	1[1]	**2**[4]	**3**	**4**	**5**
$\chi' T$ [$cm^3\,K\,mol^{-1}$] at 300 K	93	83	85	89	86
$\chi' T$ [$cm^3\,K\,mol^{-1}$] max.	894	831	770 (at 4.0 K)	904	864
$\chi' T$ [$cm^3\,K\,mol^{-1}$] at 1.8 K	894	831	688	904	864
M_{sat} [μ_B] at 1.8 K, 70 kOe	84.5	84.1	83.6	83.9	82.1

Magnetic Studies

The magnetic properties of freshly prepared polycrystalline samples of **3**–**5** were measured. For all compounds, the alternating current (ac) susceptibility was checked but showed no out-of-phase signal above 1.8 K and no frequency dependence of the in-phase component. The temperature dependence of the χT products and magnetizations for **3**–**5** are summarized in Table 2 and are very similar to the published data for **1** and **2**.[1,4]

For all of the compounds, the χT value at 300 K is significantly higher than the theoretical values for the 19 independent metal ions (66.6 $cm^3\,K\,mol^{-1}$ for g_{av} = 2.00) and then continuously increases as the temperature decreases to reach values consistent with an S = 83/2 ground state at 1.8 K (the theoretical value is 881.9 $cm^3\,K\,mol^{-1}$ for g = 2.00), provided that the susceptibility is measured with a small ac field (3 Oe at 200 Hz) rather than the more usual 1000 Oe direct current (dc) field to avoid saturation effects. The slight exception to this is **3**, for which χT reaches a maximum value of 770 $cm^3\,K\,mol^{-1}$ at 4.0 K before drop-

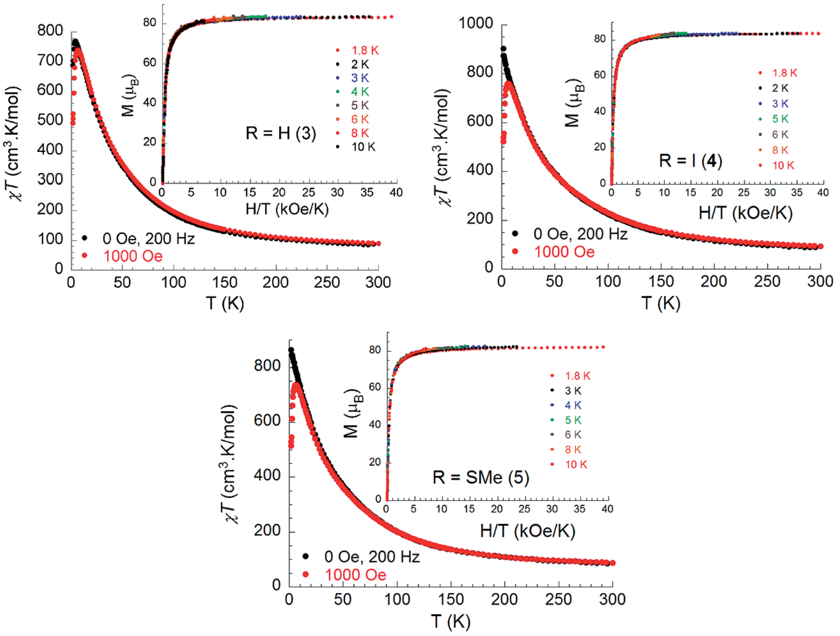

Figure 2. Temperature dependence of the χT products for **3**, **4** and **5**. Insets: reduced magnetizations at the indicated temperatures.

ping slightly to 688 $cm^3\,K\,mol^{-1}$ at 1.8 K; this is presumably the effect of weak antiferromagnetic intermolecular interactions. Ferromagnetic interactions and the $S = 83/2$ ground state for all the compounds are further confirmed by the field dependences of their magnetization below 10 K with very quick saturation of magnetization with even a small external field to reach values close to 83 μ_B (Figure 2). The almost perfect superimposition of the reduced magnetization curves at different temperatures onto a master curve for each compound indicates a lack of anisotropy (insets in Figure 2), and they are in very good agreement with Brillouin functions calculated for $S = 83/2$ and $g = 2.0$, as was also the case for **1**.[1] This demonstrates the robust nature of the central inorganic core of these [Mn_{19}] systems, as the nature of the encapsulating ligands has very little effect on the overall electronic and magnetic structure.

Summary and Conclusions

We have demonstrated the tunability of the H_3L^R ligand system based on 4-substituted 2,6-bis(hydroxymethyl)phenols by developing convenient synthetic methodologies to the ligands with R = H, Br, Ph, F, Cl, I, NO_2 and NH_2 to sit alongside the existing commercial available H_3L^{Me} and the high-yield syntheses of H_3L^{OMe} and H_3L^{Cl}.[10] By tuning the reaction conditions, new [Mn_{19}] complexes with R = H, I and SMe have been synthesized and structurally and magnetically characterized. A comparison of the data for these complexes with the data obtained for the previously published aggregates with R = Me[1] and OMe[4] indicates that changes to the ligand substituent do not result in any significant changes to the core structures or to the magnetic properties of the aggregates. All of the compounds described here exhibit ferromagnetic ground spin states consistent with the $S = 83/2$ state observed for the original [Mn_{19}] aggregate, **1**. Thus, the present work demonstrates the structural robustness of the core of the [Mn_{19}] system, which remains essentially unchanged in spite of various changes to the encapsulating ligands. This is in line with the suggestion from the DFT calculations on the [Mn_{19}] systems, which have led to the conclusion that it is the bonding parameters within the central inorganic $\{Mn^{III}{}_{12}Mn^{II}{}_7(\mu_4\text{-}O)_8\}$ core that determine the nature of the magnetic structure. Indeed, the robustness of the magnetic behaviour and electronic structure of the core with respect to encapsulating ligand functionalization is particularly appealing in view of possible applications. Thus, as synthetic routes to functionalized encapsulating ligands have been developed, it should now be possible to provide a library of further ligands to tailor the [Mn_{19}] system for attachment to a wide variety of possible substrates ranging from metal, semiconductor or insulator surfaces through to biological macromolecules with the maximum spin ground state maintained at 83/2.

Experimental Section

Ligand Synthesis

General Procedures: Reactions were performed under an argon atmosphere unless specified otherwise. Solvents were purified by standard methods before use [CH_2Cl_2 (CaH_2), MeOH (Mg), THF (Na/benzophenone)]. EtOH (HPLC grade) was used as purchased. 2-Methoxyisophthalic acid was purchased from Aldrich (85% purity; the impurity was identified as 2-methoxy-3-methylbenzoic acid, vide infra). TLC was performed with silica gel plates (Merck, 60F-254). Flash chromatography was performed with 40–63 µm SiO_2. ^1H, ^{13}C and ^{19}F NMR spectra were recorded at ambient temperature at 400 MHz with tetramethylsilane (TMS) as an internal standard (Bruker UltraShield Plus). Chemical shifts (δ) of samples in $CDCl_3$, CH_3OD or [D_6]acetone are in parts per million (ppm). The splitting patterns are designated as: s singlet, br s broad singlet, d doublet, t triplet, q quartet, and m multiplet. Coupling constants (*J*) between two nuclei separated by *n* chemical bonds are denoted in Hertz (Hz). FTIR spectra were recorded with a Nicolet 380 apparatus. HRMS spectra were recorded with an Agilent Technologies 6520 Q-TOF apparatus. Melting points were recorded with a Büchi B-540 melting point apparatus. Elemental analyses were obtained at the analytical facility of the IUT Robert Schuman, University of Strasbourg. The synthesis of 2,6-bis(hydroxymethyl)-4-chlorophenol (H_3L^{Cl}) was performed by following the literature procedure.[9] The 2,6-bis(hydroxymethyl)-4-R-phenol species (R = Br, F, H, I, NO_2) were synthesized by using improved versions of the literature procedures,[10a–10f] as described below.

Diethyl 2-Methoxyisophthalate (I): Conc. H_2SO_4 (600 µL, 11 mmol) was added to a solution of 2-methoxyisophthalic acid (940 mg, 4.78 mmol) in EtOH (45 mL). The resulting mixture was heated in the open air under reflux for 24 h. Then, the solvents were removed, and the resulting yellowish oil was dissolved in CH_2Cl_2 and dried with cotton. Purification by column chromatography (eluent: CH_2Cl_2) allowed separation of the ester **I** (1.05 g, 88 %) as a colourless oil from the monoester byproduct (vide infra). R_f = 0.5 (CH_2Cl_2). ^1H NMR ($CDCl_3$): δ = 1.39 (t, *J* = 7.2 Hz, 6 H), 3.92 (s, 3 H), 4.38 (q, *J* = 7.2 Hz, 4 H), 7.18 (t, *J* = 7.8 Hz, 1 H), 7.90 (d, *J* = 7.6 Hz, 2 H) ppm. ^{13}C NMR ($CDCl_3$): δ = 14.4, 61.5, 63.8, 123.6, 127.2, 134.9, 159.5, 165.9 ppm. Selected IR ($CDCl_3$): ṽ = 1004 (m), 1024 (m), 1148 (s), 1199 (s), 1244 (s), 1303 (s), 1465 (m), 1590 (m), 1725 (s), 2360 (w), 2982 (w) cm^{-1}. $C_{13}H_{16}O_5$ (252.27): calcd. C 61.90, H 6.39; found C 62.06, H 6.42.

Ethyl 2-Methoxy-3-methylbenzoate (byproduct): The impurity in the commercial 85 % 2-methoxyisophthalic acid is assumed to be 2-methoxy-3-methylbenzoic acid, as its ethyl ester could be isolated as a byproduct from the synthesis of **I**: white solid. R_f = 0.97 (CH_2Cl_2/AcOEt, 1:1). ^1H NMR ($CDCl_3$): δ = 1.40 (t, *J* = 7.2 Hz, 3 H), 2.32 (s, 3 H), 3.83 (s, 3 H), 4.38 (q, *J* = 7.1 Hz, 2 H), 7.05 (t, *J* = 7.6 Hz, 1 H), 7.33 (d, *J* = 7.6 Hz, 1 H), 7.63 (d, *J* = 7.8 Hz, 1 H) ppm. ^{13}C NMR ($CDCl_3$): δ = 14.4, 16.2, 61.1, 61.6, 123.6, 125.2, 129.2, 132.8, 135.1, 158.4, 166.7 ppm.

Diethyl 2-Hydroxyisophthalate (II): Compound **I** (750 mg, 2.97 mmol) was dissolved in CH_2Cl_2 (15 mL). The solution was cooled to –78 °C [acetone/CO_2(s) bath]. BBr_3 (1 M in CH_2Cl_2, 3.3 mL, 3.3 mmol) was then added dropwise. The bath was removed, and the resulting mixture was further stirred for 15 min. The bath was replaced, and water (10 mL) and HCl (1N, 5 mL) were added slowly. The organic phase was separated and further washed with H_2O (3× 15 mL), saturated $NaHCO_3$ (3× 15 mL) and H_2O (30 mL). Drying over cotton and evaporation of the solvent gave a yellow oil, which was dissolved in AcOEt and filtered over silica to yield the phenol **II** (705 mg, 99 %) as a colourless oil. R_f = 0.93 (CH_2Cl_2/AcOEt, 1:1). ^1H NMR ($CDCl_3$): δ = 1.41 (t, *J* = 7.0 Hz, 6 H), 4.41 (q, *J* = 7.0 Hz, 4 H), 6.91 (t, *J* = 7.8 Hz, 1 H), 8.04 (d, *J* = 8.0 Hz, 2 H) ppm. ^{13}C NMR ($CDCl_3$): δ = 14.4, 61.6, 117.0, 118.4, 136.2, 161.8, 167.8 ppm. Selected IR ($CDCl_3$): ṽ = 759 (s), 1024 (s), 1150 (s), 1187 (s), 1250 (s), 1439 (s), 1613 (s), 1671 (s), 1704 (s), 1732 (s), 2360 (w), 2983 (w) cm^{-1}. $C_{12}H_{14}O_5$ (238.24): calcd. C 60.50, H 5.92; found C 60.83, H 6.01.

2,6-Bis(hydroxymethyl)phenol (H_3L^H): Phenol **II** (640 mg, 2.69 mmol) was dissolved in THF (12 mL). Slowly, $LiAlH_4$ (408 mg, 10.75 mmol) was added at 0 °C. The resulting grey suspension was stirred overnight at room temperature. Et_2O (10 mL) and HCl (1 N, 15 mL) were then added slowly to the cold solution. EtOAc (100 mL) was added, and the organic phase was further washed with water (30 mL) and dried with cotton. Evaporation of the solvents yielded H_3L^H as a white crystalline solid (404 mg, 98 %). R_f = 0.49 (CH_2Cl_2/AcOEt, 1:1), m.p. 95.4 °C. ^1H NMR ([D_6]acetone): δ = 4.57 (br s, 2 H), 4.76 (s, 4 H), 6.78 (t, *J* = 7.6 Hz, 1 H), 7.12 (d, *J* = 7.6 Hz, 2 H), 8.56 (br s, 1 H) ppm. ^{13}C NMR ([D_6]acetone): δ = 62.3, 119.8, 127.1, 127.8, 154.7 ppm. Selected IR (neat): ṽ = 784 (m), 989 (s), 1008 (s), 1061 (s), 1204 (s), 1456 (s), 1594 (m), 2884 (w), 2921 (w), 3292 (m), 3401 (m) cm^{-1}. $C_8H_{10}O_3$ (154.17): calcd. C 62.33, H 6.54; found C 62.19, H 6.82.

4-Fluoro-2,6-bis(hydroxymethyl)phenol (H_3L^F):[10c] Formaldehyde (50 mL, 37 % w/w in water) was added to a solution of NaOH (5 g, 125 mmol) and 4-fluorophenol (5.6 g, 50 mmol) in a hydroalcoholic mixture (37 mL, 23 % methanol). The resulting solution was stirred for 3 d at 35 °C. Then, glacial acetic acid (7.5 mL) in water (25 mL) was added dropwise at 0 °C. The resulting solution was concentrated in vacuo. Extraction with hot EtOAc (3× 50 mL) and further drying over cotton produced an orange oil that was purified by flash chromatography (eluent EtOAc/CH_2Cl_2, 70:30 to 100:0) to yield the title fluorinated ligand H_3L^F (6.8 g, 79 %) as a yellow solid. R_f = 0.77 (AcOEt), m.p. 140 °C (ref. 137–139 °C).[9a] ^1H NMR ([D_6]acetone): δ = 4.69–4.71 (m, 2 H), 4.75 (d, *J* = 5.2 Hz, 4 H), 6.91 (d, *J* = 9 Hz, 2 H), 8.38 (s, 1 H) ppm. ^{13}C NMR ([D_6]acetone): δ = 61.6, 112.5, 112.8, 129.71, 129.78, 150.0, 156.0, 158.3 ppm. ^{19}F NMR ([D_6]acetone): δ = 50.79 (t, *J* = 9.4 Hz) ppm. Selected IR (neat): ṽ = 699 (s), 868 (s), 966 (s), 993 (s), 1014 (s), 1070 (s), 1124 (s), 1201 (s), 1245 (s), 1313 (m), 1333 (m), 1458 (s), 1482 (s), 3274 (m), 3406 (m) cm^{-1}. HRMS: calcd. for $C_8H_9FO_3$ $[M]^+$ 172.05375; found. 172.05375. $C_8H_9FO_3$ (172.16): calcd. C 55.81, H 5.27; found C 55.60, H 5.38.

4-Bromo-2,6-bis(hydroxymethyl)phenol (H_3L^{Br}): Formaldehyde (55 mL, 37 % w/w in water) was added to a solution of NaOH (5 g, 125 mmol) and 4-bromophenol (8.1 g, 47 mmol) in a water/methanol mixture (39 mL, 21 % methanol). The resulting solution was stirred overnight at 65 °C. Then, glacial acetic acid (9 mL) in water (30 mL) was added dropwise at 0 °C. The solid was collected from the resulting slurry by filtration and washed with cold water (50 mL), CH_2Cl_2 (60 mL) and cold acetone (10 mL) to yield the desired brominated phenol (10.3 g, 94 %) as a white powder. All analysis data correspond to those previously published.[10]

6-Bis(hydroxymethyl)-4-iodophenol (H_3L^I):[10d] Ligand H_3L^H (100 mg, 649 µmol) was dissolved in MeOH (4 mL), and $NaHCO_3$ (275 mg, 3.27 mmol) and benzyltrimethylammonium dichloroiodate (290 mg, 833 µmol) were added. The resulting orange suspension was stirred overnight at room temperature, and then the solvent was evaporated. The resulting solid was dissolved in EtOAc (75 mL) and H_2O (25 mL). The organic phase was further washed with water (6× 10 mL) and dried with cotton. Evaporation of the solvent gave the iodo ligand H_3L^I (168 mg, 93 %) as a yellow solid. R_f = 0.6 (CH_2Cl_2/AcOEt, 1:1), m.p. 153.1 °C. ^1H NMR ([D_6]acetone): δ = 4.69–4.74 (m, 6 H), 7.47 (s, 1 H), 8.67 (s, 1 H) ppm. ^{13}C NMR ([D_6]acetone): δ = 61.3, 81.5, 131, 135.3, 154.4 ppm. Selected IR (neat): ṽ = 697 (m), 867 (s), 929 (s), 1003 (s), 1064 (s), 1193 (s), 1206 (s), 1261 (s), 1332 (s), 1418 (s), 1455 (s), 1475 (s), 2357 (w), 2884 (w), 3307 (s), 3396 (s) cm^{-1}. $C_8H_9IO_3$ (280.06): calcd. C 34.31, H 3.24; found C 34.53, H 3.26.

2,6-Bis(hydroxymethyl)-4-nitrophenol ($H_3L^{NO_2}$):[10e] Nitrophenol (10.5 g, 75 mmol) was added to a mixture of paraformaldehyde (11, 37.8 mmol), acetic acid (45 mL) and concentrated H_2SO_4 (23 mL). The resulting suspension was heated at 50 °C for 20 h. Then, water (60 mL) was added, and the mixture was neutralized by the slow addition of ground K_2CO_3 (53 g, 0.38 mol), and stirring was maintained for 2 h. The solid was collected by filtration under vacuum and washed with cold water (50 mL), Et_2O (70 mL) and CH_2Cl_2 (30 mL) and further recrystallized from EtOH (100 mL). Purification by column chromatography (eluent CH_2Cl_2) gave 8-acetoxymethyl-6-nitro-1,3-benzodioxene (**III**; 15.8 g, 83%) as a white solid.

Compound **III** was heated to reflux in a conc. HCl/water mixture (60/90 mL) for 4 h to give the title nitro ligand $H_3L^{NO_2}$ (12.40 g, 99%) as a white solid. All analyses are in agreement with those previously reported.[10e] ^{1}H NMR ([D$_6$]acetone): δ = 4.87 (s, 4 H), 5.03 (t, J = 5.0 Hz, 2 H), 8.12 (s, 2 H), 9.71 (s, 1 H) ppm. ^{13}C NMR ([D$_6$]acetone): δ = 61.3, 122.4, 129.1, 141.4, 160.0 ppm. HRMS: calcd. for $C_8H_{10}NO_5$ [M + H]$^+$ 200.05076; found. 200.05071.

2,6-Bis(hydroxymethyl)-4-aminophenol ($H_3L^{NH_2}$): In a sealed Paar flask, Pd/C catalyst (10% w/w; 50 mg) was added to a solution of $H_3L^{NO_2}$ (405 mg, 2.03 mmol) in MeOH (20 mL). The resulting black suspension was shaken overnight at room temp. under a H_2 atmosphere (60 psi) and then filtered through paper. The resulting solution was evaporated to dryness to yield the amino ligand $H_3L^{NH_2}$ (343 mg, 99%) as a brown crystalline solid. M.p. 108.5–109.5 °C. ^{1}H NMR (MeOD): δ = 4.63 (s, 4 H), 6.64 (s, 2 H) ppm. ^{13}C NMR (MeOD): δ = 62.0, 116.3, 129.4, 140.1, 147.5 ppm. Selected IR (neat): $\tilde{\nu}$ = 879 (m), 932 (m), 988 (m), 1066 (s), 1186 (s), 1216 (s), 1273 (m), 1330 (m), 1464 (s), 1614 (m), 3280 (m), 3360 (m) cm^{-1}. HRMS: calcd. for $C_8H_{11}NO_3$ [M]$^+$ 169.07387; found. 169.07389.

2,6-Bis(hydroxymethyl)-4-(methylmercapto)phenol (H_3L^{SMe}): Formaldehyde (25 mL, 37% w/w in water) was added to a solution of NaOH (5 g, 125 mmol) and 4-(methylmercapto)phenol (2.8 g, 20 mmol) in a hydroalcoholic mixture (16 mL, 38% methanol). The resulting solution was stirred overnight at 50 °C. Glacial acetic acid (4.4 mL) in water (8 mL) was then added dropwise at 0 °C to pH 5–6, and the resulting solution was concentrated in vacuo. The resulting orange solid was dissolved in EtOAc (50 mL) and H_2O (30 mL). The organic phase was then dried with cotton wool to afford a white solid, which was purified by flash chromatography (eluent: CH_2Cl_2/MeOH, 100:0 to 95:5) to yield the methylmercapto ligand H_3L^{SMe} (2.9 g, 73%) as a white solid. R_f = 0.36 (CH_2Cl_2/MeOH 95:5), m.p. 90–91 °C. ^{1}H NMR ([D$_6$]acetone): δ = 2.40 (s, 3 H), 4.60 (t, J = 5.4 Hz, 2 H), 4.75 (d, J = 5.6 Hz, 4 H), 7.15 (s, 2 H), 8.53 (s, 1 H) ppm. ^{13}C NMR ([D$_6$]acetone): δ = 17.9, 61.84, 61.97, 127.6, 128.9, 153.1 ppm. Selected IR (neat): $\tilde{\nu}$ = 875 (s), 1005 (s), 1063 (s), 1205 (s), 1262 (m), 1337 (m), 1423 (s), 1435 (s), 1455 (s), 1476 (s), 3280 (m), 3368 (m) cm^{-1}. HRMS: calcd. for $C_9H_{12}O_3S$ [M]$^+$ 200.05071; found. 200.05076.

Synthesis of Complexes 3–5

General Details: All reactions were performed under aerobic conditions by using the ligands described above and commercially available reagents, which were used as received without further purification. Elemental analyses (CHN) were performed with a Vario EL elemental analyzer. FTIR spectra were recorded with a Perkin–Elmer Spectrum One spectrometer with samples prepared as KBr pellets.

Caution! *Although no such tendency was observed during the present work, azides (N_3) are potentially explosive and should be handled with care and in small quantities.*

$[Mn^{III}_{12}Mn^{II}_7(\mu_4\text{-}O)_8(\mu_3\text{-}Cl)_7(\mu_3\text{-}OMe)(HL^H)_{12}(MeOH)_6]Cl_2\cdot 16H_2O\cdot 10MeOH\cdot MeCN$ (3): A slurry of $MnCl_2\cdot 4H_2O$ (0.1 g, 0.5 mmol), Et_3N (0.08 g, 0.8 mmol) and H_3L^H (0.077 g, 0.5 mmol) in MeCN (15 mL) and MeOH (3 mL) was stirred for 2 h under ambient conditions to afford a dark brown solution, which was then filtered. Dark brown blocks of **3** were obtained overnight and dried in vacuo, yield 64% (based on Mn). $[C_{103}H_{123}Cl_7Mn_{19}O_{51}]Cl_2\cdot 13H_2O\cdot MeCN$ (3815.2): calcd. C 33.06, H 4.02, N 0.37; found C 33.09, H 4.19, N 0.32. Selected IR data (KBr): $\tilde{\nu}$ = 474 (w), 548 (m), 644 (s), 810 (m), 862 (w), 985 (m), 1024 (m), 1160 (m), 1226 (m), 1251 (m), 1384 (s), 1470 (s), 1633 (w), 2930 (m), 3370 (br, s) cm^{-1}.

The same reaction in the presence of NaN_3 afforded a brown solution, which failed to yield crystalline material for further analysis.

$[Mn^{III}_{12}Mn^{II}_7(\mu_4\text{-}O)_8(\mu_3\text{-}N_3)_8(HL^I)_{12}(MeOH)_4(H_2O)_2](O_2CH)_2\cdot 16MeOH\cdot 10MeCN$ (4): A slurry of $MnCl_2\cdot 4H_2O$ (0.04 g, 0.2 mmol), NaN_3 (0.039 g, 0.6 mmol), $NaO_2CMe\cdot 3H_2O$ (0.021 g, 0.15 mmol) and H_3L^I (0.14 g, 0.5 mmol) in MeCN (15 mL) and MeOH (3 mL) was stirred at room temperature for 1.5 h and then heated at reflux for 2.5 h, after which the dark brown reaction mixture was slowly cooled and filtered. Dark brown crystals of the title cluster were obtained after 2 d, washed with a small amount of MeCN and dried in air over several days, yield 25% (based on Mn). $[C_{102}H_{204}I_{12}Mn_{19}N_{24}O_{50}](O_2CH)_2\cdot 5MeCN\cdot 5MeOH$ (5589.0): calcd. C 26.02; H 2.66; N 7.39; found C 26.05; H 2.51; N 7.23. Selected IR (KBr pellet): $\tilde{\nu}$ = 527 (m), 612 (s), 636 (s), 761 (m), 881 (m), 964 (w), 996 (m), 1012 (m), 1080 (w), 1199 (s) 1221 (m), 1264 (s), 1312 (m), 1384 (w), 1417 (w), 1464 (vs), 1501 (w), 1607 (m), 2060 (vs, N_3), 2820 (m), 2926 (m), 3024 (m), 3060 (m), 3361 (s, br) cm^{-1}.

$[Mn^{III}_{12}Mn^{II}_7(\mu_4\text{-}O)_8(\mu_3\text{-}Cl)_{7.7}(\mu_3\text{-}OMe)_{0.3}(HL^{SMe})_{12}(MeOH)_6]Cl_2\cdot 27MeCN$ (5): A slurry of $MnCl_2\cdot 4H_2O$ (0.06 g, 0.3 mmol), Et_3N (0.041 g, 0.4 mmol) and H_3L^{SMe} (0.06 g, 0.3 mmol) in MeCN (15 mL) and MeOH (3 mL) was stirred for 2 h under ambient conditions to afford a dark brown solution, which was then filtered. Dark brown blocks of **5** were obtained overnight and dried in vacuo, yield 64% (based on Mn). $[C_{114.3}H_{144.9}Cl_{7.7}Mn_{19}O_{50.3}S_{12}]\text{-}Cl_2\cdot 7H_2O\cdot 2.5MeCN$ (4324.8): calcd. C 32.99, H 3.85, N 0.75, S 8.91; found C 32.88, H 3.64, N 0.89, S 8.96. Selected IR data (KBr pellet): $\tilde{\nu}$ = 550 (s), 622 (s), 674 (s), 773 (s), 875 (w), 1020 (s), 1109 (w), 1244 (s), 1277 (m), 1446 (s), 1462 (s), 1587 (m), 2918 (m), 3207 (br, s) cm^{-1}. The same reaction in the presence of NaN_3 afforded a brown solution, which failed to yield crystalline material for further analysis.

X-ray Data Collection and Structure Refinement: The data for **3** and **4** were collected at 180(2) K with a Stoe IPDS II diffractometer by using graphite-monochromated Mo-K_α radiation. Crystals of **5** were invariably small and weakly-diffracting, and the dataset was recorded at 150(2) K with a Bruker SMART Apex diffractometer on the SCD beamline of the ANKA synchrotron source, Karlsruhe, Germany with Si-monochromated radiation with λ = 0.8000 Å. The data were corrected for absorption, the structures were solved by direct methods (SHELXTL), and full-matrix least-squares refinement against F^2 (all data) was performed with SHELXL-2013.[13] All ordered non-H atoms were refined anisotropically. The face-bridging ligands on the threefold axes in **3** and **5** were a disordered superposition of chloride and methoxo ligands, and these were assigned relative occupancies of 50:50 and 85:15, respectively. Disordered lattice solvent molecules and counterions that could not be refined satisfactorily with partial occupancies were handled by using the SQUEEZE option in PLATON.[14] The crystallographic data and structure refinement details for **3**–**5** are listed in Table 3.

CCDC-953780 (for **3**), -953782 (for 4) and -922474 (for **5**) contain the supplementary crystallographic data for this paper. These data can be obtained free of charge from The Cambridge Crystallographic Data Centre via www.ccdc.cam.ac.uk/data_request/cif.

Table 3. Crystallographic data for **3**–**5**.

	$Mn_{19}H$ (**3**)	$Mn_{19}I$ (**4**)	$Mn_{19}SMe$ (**5**)
Formula	$C_{115}H_{198}Cl_9Mn_{19}NO_{77}$	$C_{140}H_{204}I_{12}Mn_{19}N_{34}O_{70}$	$C_{168.3}H_{225.9}Cl_{9.7}Mn_{19}N_{27}O_{50.3}S_{12}$
Mr	4189.65	6050.02	5204.51
Crystal system	trigonal	monoclinic	cubic
Space group	$R\bar{3}$	$P2_1/n$	$Pa\bar{3}$
T [K]	180(2)	180(2)	150(2)
a [Å]	20.3770(8)	23.3872(12)	27.5286(11)
b [Å]	20.3770(8)	16.8363(5)	27.5286(11)
c [Å]	37.263(2)	26.1412(13)	27.5286(11)
α [°]	90	90	90
β [°]	90	94.774(4)	90
γ [°]	120	90	90
V [Å^3]	13399.6(10)	10257.5(8)	20861.8(14)
Z	3	2	4
$\rho_{calcd.}$ [g cm^{-3}]	1.558	1.959	1.659
μ [mm^{-1}]	1.510	3.019	1.927
$F(000)$	6417	5906	10660
λ [Å]	0.71073	0.71073	0.8000
Reflections collected	34489	58795	91393
Unique data	6320	18779	7396
R_{int}	0.0656	0.0633	0.0344
Data with $I > 2\sigma(I)$	5044	11301	6087
Parameters/restraints	340/14	1127/32	292/21
S on F^2 (all data)	0.989	0.918	1.108
wR_2 (all data)	0.1015	0.1324	0.2059
R_1 [$I > 2\sigma(I)$]	0.0484	0.0540	0.0603
Largest residuals [e Å^{-3}]	+0.40/–0.45	+1.60/–1.02	+1.03/–0.52

Magnetic Measurements: The magnetic susceptibility measurements were obtained with a Quantum Design MPMS-XL superconducting quantum interference device (SQUID) magnetometer over the temperature range 1.8–300 K first with a dc field of 1000 Oe and then in zero dc field with an oscillating ac field of 3 Oe and an ac frequency of 200 Hz. The magnetization measurements were made over a temperature range of 1.8–300 K with dc applied fields from 0 to 70 kOe. The measurements of M vs. H at 100 K were additionally used to check for the presence of ferromagnetic impurities, which were found to be absent. All measurements were performed on fresh finely ground crystalline samples restrained in grease, and the magnetic data were corrected for the sample holder.

Acknowledgments

This work was supported by the Deutsche Forschungsgemeinschaft (DFG) (Center for Functional Nanostructures) and Centre National de la Recherche Scientifique (CNRS). The authors acknowledge the Synchrotron Light Source ANKA for provision of instrumentation on the SCD beamline. Dr. Gernot Buth is thanked for experimental assistance. S. M. is thankful to Alain Hazemann of the IUT Robert Schuman (Unistra) for elemental analyses.

---

[1] A. M. Ako, I. J. Hewitt, V. Mereacre, R. Clérac, W. Wernsdorfer, C. E. Anson, A. K. Powell, *Angew. Chem. Int. Ed.* **2006**, *45*, 4926–4929; *Angew. Chem.* **2006**, *118*, 5048–5051.

[2] O. Waldmann, A. M. Ako, H. U. Güdel, A. K. Powell, *Inorg. Chem.* **2008**, *47*, 3486–3488.

[3] E. Ruiz, T. Cauchy, J. Cano, R. Costa, J. Tercero, S. Alvarez, *J. Am. Chem. Soc.* **2008**, *130*, 7420–7426.

[4] a) A. M. Ako, M. S. Alam, S. Mameri, Y. Lan, M. Hibert, M. Stocker, P. Müller, C. E. Anson, A. K. Powell, *Eur. J. Inorg. Chem.* **2012**, 4131–4140.

[5] T. Glaser, I. Liratzis, A. M. Ako, A. K. Powell, *Coord. Chem. Rev.* **2009**, *253*, 2296–2305, and references cited therein.

[6] C. Lampropoulos, K. A. Abboud, T. C. Stamatatos, G. Christou, *Inorg. Chem.* **2008**, *47*, 813–815.

[7] e.g.M. Mannini, P. Sainctavit, R. Sessoli, C. Cartier dit Moulin, F. Pineider, M.-A. Arrio, A. Cornia, D. Gatteschi, *Chem. Eur. J.* **2008**, *14*, 7530–7535, and references cited therein.

[8] a) M. Evangelisti, E. K. Brechin, *Dalton Trans.* **2010**, *39*, 4672–4676, and references cited therein; b) S. Nayak, M. Evangelisti, A. K. Powell, J. Reedijk, *Chem. Eur. J.* **2010**, *16*, 12865–12872.

[9] a) Y.-Z. Zheng, M. Evangelisti, R. E. P. Winpenny, *Angew. Chem. Int. Ed.* **2011**, *50*, 3692–3695; *Angew. Chem.* **2011**, *123*, 3776; b) Y. Wang, W. Li, S. Zhou, D. Kong, H. Yang, L. Wu, *Chem. Commun.* **2011**, *47*, 3541–3543; V. Ozdemir, B. Williams-Jones, S. J. Glatt, M. T. Tsuang, J. B. Lohr, C. Reist, *Nature Biotechnol.* **2006**, *24*, 942–946.

[10] a) A. A. Moshfegh, B. Mazandarini, A. Nahid, G. H. Hakimelahi, *Helv. Chim. Acta* **1982**, *65*, 1229–1232; b) R. S. Drago, M. J. Desmond, B. B. Corden, K. A. Miller, *J. Am. Chem. Soc.* **1983**, *105*, 2287–2296; c) P. D. Hampton, Z. Bencze, W. Tong, C. E. Daitch, *J. Org. Chem.* **1994**, *59*, 4838–4843; d) G. T. Crisp, P. D. Turner, *Tetrahedron* **2000**, *56*, 407–415; e) J. De Mendoza, P. M. Nieto, P. Prados, C. Sánchez, *Tetrahedron* **1990**, *46*, 671–682; f) T. Routasalo, J. Helaja, J. Kavakka, A. M. P. Koskinen, *Eur. J. Org. Chem.* **2008**, 3190–3199.

[11] C. Hansch, A. Leo, *Substituent Constants for Correlation Analysis in Chemistry and Biology*, Wiley-Interscience, New York, **1979**.

[12] A. M. Ako, B. Burger, Y. Lan, V. Mereacre, R. Clérac, G. Buth, S. Gómez-Coca, E. Ruiz, C. E. Anson, A. K. Powell, *Inorg. Chem.* **2013**, *52*, 5764–5774.

[13] G. M. Sheldrick, *Acta Crystallogr., Sect. A* **2008**, *64*, 112–122.

[14] P. van der Sluis, A. L. Spek, *Acta Crystallogr., Sect. A* **1990**, *46*, 194–201.

Received: May 15, 2014
Published Online: July 24, 2014